

Terrain Based Parameter Optimization for Zero-Velocity Update Inertial Based Navigation Solutions[†]

Taylor Knuth ^{1,2*} and Paul Groves ²¹ Northrop Grumman Corporation; taylor.knuth@ngc.com² University College London

* Correspondence: taylor.knuth.18@ucl.ac.uk.

[†] Presented at the European Navigation Conference 2024, ESA ESTEC, May 22, 2024.

Abstract: This paper demonstrates the benefits of adapting Zero-Velocity Update (ZVU) algorithms in foot-mounted pedestrian inertial navigation by finely tuning the algorithm to account for the type of terrain over which the pedestrian travels. Conventional ZVU algorithms for foot-mounted inertial navigation are designed for indoor use and do not account for differences from various terrains. Different terrains affect the natural pedestrian gait and how zero-velocity intervals (ZVIs) are identified. By tuning the algorithm to account for accelerometer and gyroscope magnitude and walking cycle duration across four terrains (concrete, grass, pebble and sand) the accuracy is improved up to 31.04%, dependent on the terrain, and viable for outdoor use.

Keywords: Zero-velocity update; pedestrian inertial navigation; terrain-dependent

1. Introduction

Inertial Measurements Units (IMU) collect data that is extracted for navigation solutions. The simplest models are examples of dead reckoning, which is any method of navigation that sums measurements of distance travelled or integrates measurements of velocity to calculate distance via known inputs or estimated user step length and a heading measurement [1]. In pedestrian dead reckoning (PDR), position and heading are derived by measuring specific force and angular rate with a microelectromechanical systems (MEMS) IMU attached in a minimally invasive manner to not disrupt the natural gait [2]. With a known starting point, heading, and distance an estimation of each step and position of the pedestrian can be calculated. However, there are limitations involved when relying solely on PDR navigation. These limitations include an increase in error bounds, or the area where it is statistically possible to be located for all detected steps [3], the magnetometer and gyroscope heading output is susceptible to magnetic interference and without heading corrections the solution succumbs to magnetic disturbances and drift [4], and poor-quality sensors used in MEMS IMU lead to drift in the heading solution.

Foot-mounted inertial navigation can achieve high accuracy from poor quality sensors by performing zero-velocity updates (ZVU) every step [5]. ZVUs keep sensors calibrated and minimize drift in the position solution. To get the best performance, the ZVU algorithm needs to be carefully tuned [3]. ZVU algorithms are used for pedestrian navigation by collecting inertial data with an IMU and identifying zero-velocity intervals [6] when the IMU is briefly stationary. Stationary pedestrian detection relies on the walking cycle where the foot is constantly accelerating or decelerating. The walking cycle is divided into the stance and swing phase [7]. The stance phase is the period of time when the foot is in contact with the ground, from the heel strike to the heel release [8]. The swing phase is the duration of the foot leaving the ground until the same foot touches the ground again [9]. Figure 1 is an example of one cycle of the two phases in the walking cycle. The

Citation: To be added by editorial staff during production.

Academic Editor: Firstname Last-name

Published: date



Copyright: © 2024 by the authors. Submitted for possible open access publication under the terms and conditions of the Creative Commons Attribution (CC BY) license (<https://creativecommons.org/licenses/by/4.0/>).

stationary detection occurs during the stance phase. The stationary period is also known as a zero-velocity interval (ZVI) and historically this was assumed to be about 0.2 seconds within the entire walking cycle of about 1.14 seconds [10]. When the accelerometer or gyroscope measurements are below a test quantity, computed from a specified moving window of time, the foot is assumed to be stationary. One accepted threshold value is below the magnitude of 1.239 m/s^2 of the MEMS accelerometers, where the value of gravity is factored out of consideration [11]. The threshold value comes from empirical data and the calculation of acceleration from the average force of the heel strike [12].

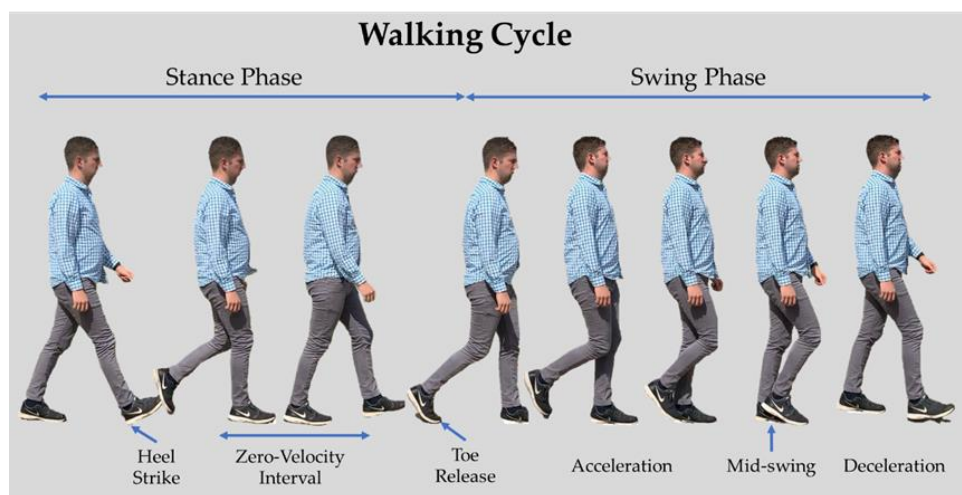


Figure 1. Demonstration of the walking cycle for the stance and swing phase.

In addition to ZVU-aided inertial navigation algorithms, a zero angular rate update (ZARU) can be performed in conjunction with ZVUs. ZARUs are similar to ZVUs, because they help keep sensors calibrated and aligned during the walking cycle when the angular rate measured is below a specific threshold. ZARUs can be utilized in addition to a ZVU, but not as an independent inertial navigation algorithm [3].

The identification of ZVIs and the zero-angular rate during the walking cycle is difficult because the foot tends to rotate during the stance phase, and varies between individual, shoe style, and terrain. Thus, some parts of the foot are more stationary than others. Identifying the ZVIs and zero-angular rates is accomplished using MEMS IMUS, similar to how context detection is used to decipher pedestrian activities [13]. Previous work has shown that in addition to using context detection for identifying pedestrian behavior, data recorded from MEMS IMUs can determine varying terrains over which a pedestrian traveled. This suggests that the walking cycle and natural gait of a pedestrian is affected by the terrain [14]. Studies have shown that there are changes in pedestrian speed across differing terrains [11, 15-16], suggesting that the natural gait of the walking cycle is affected. Most work on foot-mounted inertial navigation has been conducted indoors on hard surfaces [17-18], but a reliable system needs to work effectively both indoors and outdoors on a variety of different surfaces.

Similar to a human's ability to use sensory awareness in determining terrain while walking due to differences experienced in the gait cycle, a ZVU navigation solution must account for this difference. Human sensory awareness determines changes in terrain type while walking and work by Knuth and Groves verified that inertial data can be used to differentiate between terrains with 99.24% accuracy using a k-Nearest Neighbor machine learning algorithm [14]. If the natural gait is affected, then the differences will be recorded by the IMU, and ZVU navigation algorithms should be tuned for differences to the gait.

Existing ZVU and ZARU navigation algorithms are limited by using predetermined thresholds and tuning parameters to determine accuracy, such as acceleration-moving variance detectors [19], acceleration-magnitude detectors [20], angular rate energy

detectors [21], and duration of ZVI [10]. Conventionally, these parameters are used regardless of terrain type. If differences are experienced while walking across different terrains, then these differences affect ZVU-aided inertial navigation solutions.

In order to determine how differences in terrain affect the navigation solution, an investigation on how parameters to existing ZVU and ZARU algorithms are used is needed. Furthermore, an examination into additional parameters is required to accommodate the differences in terrain from sensory awareness. For comparisons OpenShoe, an opensource ZVU-aided inertial navigation algorithm for use with foot-mounted IMUs, is used throughout as a navigation algorithm [22] and modified to include terrain-dependent parameters. For ZVUs, the threshold is calculated from the magnitude of the three-axis accelerometer during the ZVI. In this paper, a test statistic is used to account for gravity in the accelerometer magnitude threshold. Equation 1 converts the raw data into test data:

$$\text{Accelerometer Magnitude} = \left| \sqrt{x^2 + y^2 + z^2} - 9.81 \right|. \quad (1)$$

The ZARU threshold is calculated from the magnitude of the three-axis gyroscope during the stance phase. Finally, the last parameters are the time of a complete cycle and duration of the ZVI. This accounts for the time between each step, including the ZVI, and sets a timing threshold where a step is not measured without a wait period. A visualization of the thresholds during the walking cycle is shown in Figure 2 by applying a moving average filter to help with conceptualization, the data was collected from a single user using a MEMS IMU to demonstrate the walking cycle on concrete.

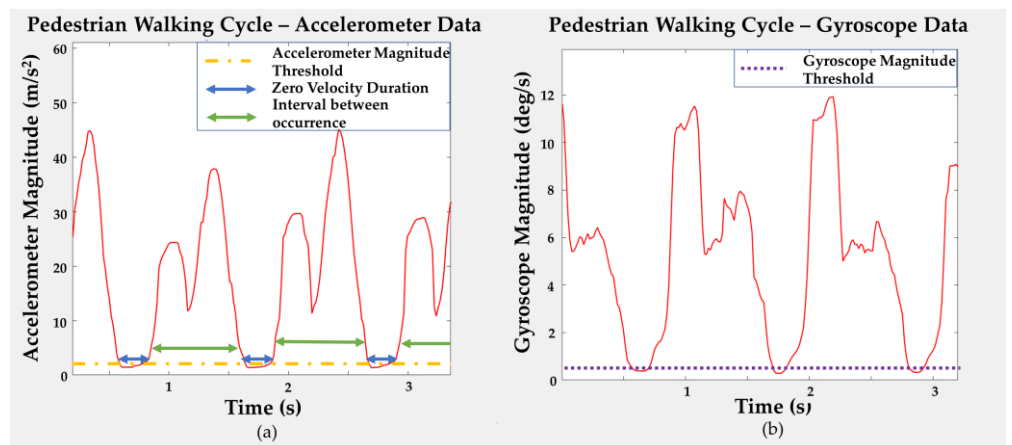


Figure 2. Pedestrian walking cycle demonstration on concrete. (a) Visualization of ZVU parameters for accelerometer magnitude, zero-velocity duration, and duration between occurrences for accelerometer data. (b) Visualization of ZARU parameter for gyroscope magnitude.

2. Materials and Methods

Four terrains were used in previous work and were successfully identified using IMU data: concrete, grass, pebble and sand [14]. For algorithm tuning across different terrains, an IMU is attached to the foot of the user for greater sensitivity when recording the inertial data. To reduce impact on pedestrian gait, an IMU was placed on top of the right shoe, shown in Figure 3. Attaching the IMU to the surface of the shoe, above the toes, provides the most consistent step and ZVI detection [23–24] when compared to placement on the ankle or heel. Attaching the IMU to the ankle requires a support structure that limits the motion of the foot and when the IMU is attached to the heel, the straps used to secure the IMU wrap under the arch of the foot and affect the natural gait.



Figure 3. Placement of an IMU on top of right shoes above the toes.

Data was collected using a six degree of freedom (DOF) IMU from Inertial Elements [25]. Inertial Element’s IMU is low-cost and compact, the sensor specifications are in Table 1. IMU data is recorded via Bluetooth to an Android app, OsmiumScope. The IMU is attached using Velcro above the toe of the shoe to reduce impact on the natural gait. By attaching the IMU with Velcro, there are no straps under the arch of the foot to alter each footstep or any casing at the heel that affects the balance of the user and changes the gait. The adhesive Velcro strips cover the base of the IMU housing, the larger contact area reduces the likelihood of the IMU shifting during data collection and affecting the measurements. The IMU records data along three orthogonal axes: X; Y; and Z for both accelerometers and gyroscopes. The collected data on the mobile phone was exported for processing.

Table 1. Inertial Elements MIMU22BLPX sensor specifications

Sensor	Axis	Bias Stability (mg)	Velocity Random Walk (m/s/√hr)
Accelerometer	X	0.051	0.079
	Y	0.063	0.08
	Z	0.056	0.073
	Axis	Bias Stability (°/hr)	Angle Random Walk (°/√hr)
Gyroscope	X	4.76	0.381
	Y	4.49	0.366
	Z	4.62	0.378

Tuning data was collected on four terrains using an IMU attached to athletic trainers. A single user wearing athletic trainers was used for data collection, thus eliminating gait variation. Test locations are all in England. Tuning data for the concrete and grass terrains was collected at Royal Air Force Mildenhall (RAF M) on a concrete running track and grass field. Data used for tuning the pebble terrain was collected at Chesil Beach. The sand tuning data was collected at Weymouth Beach. The beach terrains are defined using the Wentworth Scale [26], based on the grain size. Chesil Beach is a pebble beach with aggregates of 30 – 200 mm in diameter and Weymouth beach is a very fine to fine sand with grains of 0.0625 to 0.25 mm in diameter. Each beach and their respective grain types are shown in Figure 4.



Figure 4. (a) Weymouth Beach in England. (b) Sand at the beach. (c) Chesil Beach in England. (d) Pebbles at Chesil Beach.

Tuning for the algorithm was performed by manually identifying the ZVIs and zero angular rate intervals across the terrains. Initial analysis indicated that the less firm the terrain was, the more variation in the threshold value. Figure 5 shows data from the test statistic

accelerometer magnitude of four terrains. The ZVIs are noisier for the sand and pebble terrains, whereas the concrete and grass terrains are more stable.

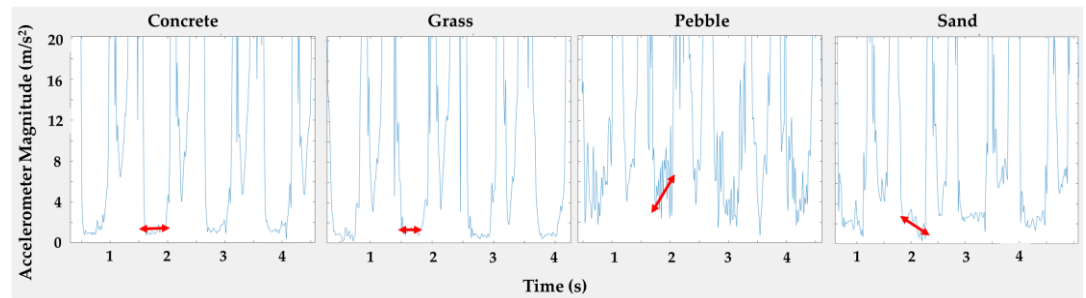


Figure 5. Visualization of ZVI slope for four different terrains.

The values for each parameter were determined from manual tuning and data selection. The visual inspection of each stance phase was conducted by selecting the start of the ZVI following the heel strike. A second point was selected at the end of the ZVI before the magnitude increases due to the toe release. All magnitude and time data between the two points was exported, saved for each footstep from the tuning data and averaged to create a threshold value. The time between the first and second selected points is saved and a difference is calculated for the ZVI duration. The difference is saved for each set of selected points and averaged for the tuning data for the ZVI duration of the tested terrain. An additional difference is calculated between the second point selected and the following first point of the next ZVI. This difference is saved for the tuning data and averaged for the duration of the walking cycle, excluding the ZVI. Finally, the process is repeated for the gyroscope magnitude data to determine the zero angular rate threshold. The average values of the four parameters of the terrains is shown in Table 2. The four parameters comprise the tuning for the algorithm used for pedestrian navigation.

Table 2. The average parameter values for tuning the ZVU algorithm for four separate terrains.

Tuning Parameter	Concrete	Grass	Pebble	Sand
Zero Angular Rate Max Threshold (deg/s)	0.256	0.386	0.568	0.303
Zero Velocity Max Threshold (m/s ²)	1.422	1.485	4.351	1.815
ZVI Duration (s)	0.112	0.119	0.140	0.187
Walking Cycle Duration – excluding ZVI (s)	1.040	1.122	1.154	1.140

One standard deviation is then applied to each calculated average for the parameter threshold values to account for missed step detections in the walking cycle. The standard deviation for each parameter is shown in Table 3. The missed detections are attributed to variations in the ground, especially for softer terrains, where the ground gives way under each footstep. The final threshold values for each parameter are in Table 4. The threshold value for the zero-velocity threshold for concrete of 1.42 ± 0.21 m/s² is within the standard deviation of the 1.239 m/s² single indoor threshold accepted value from literature.

Table 3. Standard deviations of terrain-dependent parameters.

Tuning Parameter	Concrete	Grass	Pebble	Sand
Zero Angular Rate Max Threshold (deg/s)	0.045	0.098	0.428	0.135
Zero Velocity Max Threshold (m/s ²)	0.213	0.624	1.434	1.262
ZVI Duration (s)	0.025	0.043	0.060	0.057
Duration of Walking Cycle – excluding ZVI (s)	0.032	0.049	0.085	0.077

Table 4. ZVU algorithm parameter threshold values for four terrains and an indoor threshold.

Tuning Parameter	Concrete	Grass	Pebble	Sand	Indoor
Zero Angular Rate Max Threshold (deg/s)	0.301	0.484	0.996	0.439	0.555
Zero Velocity Max Threshold (m/s ²)	1.635	2.108	5.785	3.077	1.239
ZVI Duration (s)	0.086	0.076	0.080	0.130	0.080
Duration of Walking Cycle – excluding ZVI (s)	1.009	1.073	1.069	1.063	1.000

The ZVU is performed whenever the test statistic is below the threshold. The algorithm waits for the ZVI and duration of the walking cycle before searching again for a value below the threshold. The ZVI and walking cycle vary for each terrain, so wait time is terrain-dependent. This process is repeated for the ZARU. The magnitude thresholds for the accelerometers and gyroscopes are synched and the ZARU is identified when the test statistic is below the threshold of the gyroscope magnitude. If a ZVI and zero angular rate instance occur within one ZVI duration, heading and position are updated.

The differences in the measured threshold values are consistent with sensory awareness that different terrains affect the natural gait, thus separate threshold values need to be considered when using a ZVU algorithm.

When testing the algorithm, new data was collected across the four terrains. The threshold value used in literature of 1.239 m/s² is derived from Schwartz’s work on walking patterns of “normal” males [12] as well as Gast’s work on walking speed on different terrains [11]. OpenShoe assumes the walking surface to be firm without uneven imperfections. These assumptions are similar to concrete and thus accepted as a suitable comparison for the concrete terrain, as majority of work in ZVU-aided inertial navigation focuses on indoor navigation. The other terrains considered are not always on a firm foundation, meaning the ground on which the user walks can give way under each footstep. Additionally, the surfaces of the three other terrains may exhibit unevenness or imperfections.

To test the algorithm, datasets were collected at four locations: RAFM– concrete; Red Lodge Community Hall – grass; Aldeburgh Beach – pebble; and Southwold Beach – sand. Figure 6 is a picture of each terrain at the test locations.

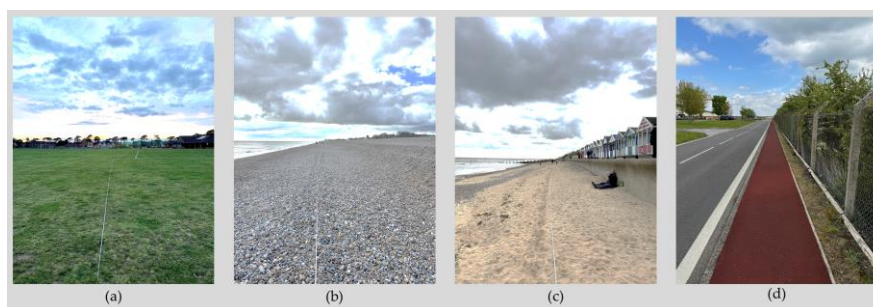


Figure 6. Test Terrains: (a) Grass at RAFM (b) Pebble at Aldeburgh Beach. (c) Sand at Southwold Beach. (d) Concrete track at RAFM.

To compare the calculated terrain thresholds against existing ZVU algorithms the opensource OpenShoe ZVU algorithm is used as a baseline. For an accurate comparison, a 100m straight line was measured with surveying tape. A single user collected data along the straight line to eliminate heading errors. Data was collected at 125 Hz with the Inertial Elements IMU for five tests at each location. The collected data was post-processed and analyzed with the OpenShoe algorithm using existing threshold values and compared to the OpenShoe algorithm using terrain-specific parameters. The 100m is a truth reference distance against which the default ZVU-aided inertial navigation algorithm is compared. Additionally, the ZVU-aided inertial navigation algorithm with terrain-dependent parameters is compared to the 100m reference. Comparing both ZVU algorithms to the 100m reference distance shows how each algorithm performs in calculating distance traveled.

3. Results

The ZVU algorithm identifies the first instance under the threshold value in the ZVI and waits the time interval before searching for another instance. Occasionally steps are missed due to time constraints or the magnitude never crossing below the threshold. Figure 7 highlights steps using the ZVU algorithm on pebble terrain. Figure 7(a) uses single threshold values not tuned to the terrain - missing five steps. Figure 7(b) uses terrain-specific threshold values and identifies all nine steps.

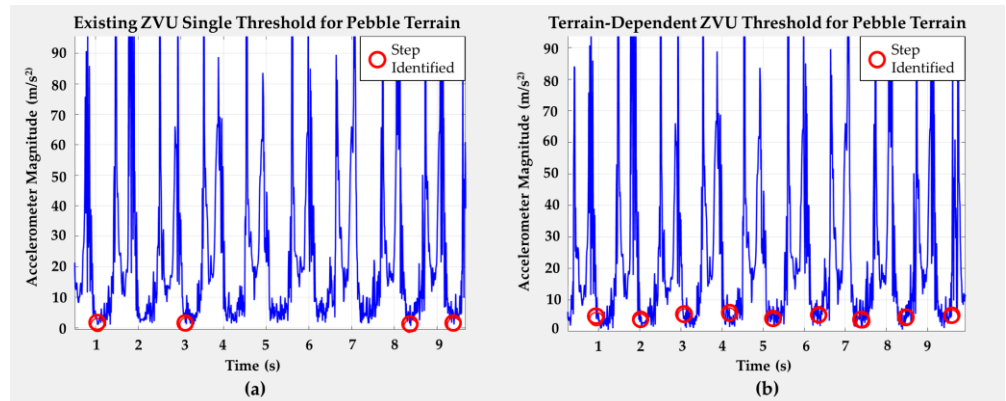


Figure 7. Pebble terrain step identification (a) ZVU single threshold identification. (b) ZVU threshold identification using terrain-dependent pebble parameters.

The baseline ZVU algorithm was run for all terrains using the single indoor threshold value across each test and terrain. The ZVU algorithm was then run for all terrains with terrain-specific parameter values. The distance measured using ZVU-aided inertial navigation from each test is compared to each other and the 100m reference. A comparison between the terrain-specific thresholds and the indoor single threshold is calculated using root mean square error (RMSE) from the measured distances in Equation 2:

$$RMSE = \sqrt{(f - o)^2}, \tag{2}$$

where f is the measured distance of each test, and o is the 100m reference. The RMSE comparisons between the terrain-specific parameters and single threshold is in Table 5. Using the single threshold for concrete results in a 4.601m error. This is the most accurate result for the single threshold and consistent with concrete terrain using terrain-dependent parameters. Concrete is a hard surface similar to indoor surfaces on which the single threshold was tuned. For the other terrains the single threshold yields distance errors of 29.351, 35.137 and 36.253m. Using terrain-dependent thresholds yields an RMSE below 8.239m for all terrains. The improved accuracy of distance measured using terrain-dependent thresholds versus an indoor threshold is in Table 5 and calculated in Equation 3:

$$\text{Terrain Threshold Improvement} = \left| \frac{RMSE_t - RMSE_i}{RMSE_t - 100} \right|, \tag{3}$$

where $RMSE_t$ is the RMSE value for each terrain-dependent threshold, $RMSE_i$ is the RMSE value using the indoor threshold and 100 is the reference distance.

Table 5. RMSE computed using ZVU-aided inertial navigation across five 100m lengths on each of four different terrains using terrain-dependent and single ZVU thresholds.

Terrain	RMSE with terrain-dependent thresholds (m)	RMSE with indoor threshold (m)	Terrain-Dependent Percent Improvement (%)
Concrete	1.491	4.601	3.157
Grass	2.506	29.351	27.531
Pebble	8.239	35.137	29.316
Sand	7.560	36.253	31.036

Using the single indoor threshold parameters, a distance of 95.399m was calculated for the concrete terrain and performed worse for each subsequent terrain. The terrain-dependent parameters are tuned to the specific terrains. The terrain data was tested using the parameters for the other terrains; for example, the pebble data was tested using concrete parameters. This was repeated for every permutation of terrain and terrain parameters. Table 6 shows the distances when terrain data is tested using parameters for other terrains. The ZVU algorithm using the pebble and sand terrain parameters is more likely to identify steps because the threshold is larger, but when the sand and pebble data is tested using the concrete or grass parameters the RMSE calculated is above 18.355m.

Table 6. RMSE (m) with varying thresholds across four terrains.

		Threshold				
		Concrete	Grass	Pebble	Sand	Indoor
Terrain Data	Concrete	1.491	2.334	0.733	0.730	4.601
	Grass	10.361	2.506	0.745	0.750	29.351
	Pebble	18.818	19.889	8.239	12.240	35.137
	Sand	24.063	18.355	3.583	7.560	36.253

4. Conclusion

In this work, fine tuning a ZVU-aided inertial navigation algorithm with terrain-specific threshold parameters demonstrated that terrain-dependent tuning affects the navigation solution. Using terrain-specific threshold values of four parameters (accelerometer and gyroscope magnitudes and durations of the ZVI and walking cycle) instead of values optimized for indoor use on hard surfaces, improved navigation accuracy. The terrain-dependent thresholds improved the distance measured by: 3.157, 27.531, 29.316 and 31.036% across concrete, grass, pebble and sand terrains. The accuracy was better on concrete and grass because as pedestrians walk on sand or pebble terrains, the terrain gives way causing more variation in accelerometer and gyroscope magnitude during each step.

Future investigation is needed to determine if reducing the number of terrain classes to two, hard and soft, can improve accuracy and reduce the computational load of ZVU algorithms. Further investigation is recommended to understand the algorithm in real time as the pedestrian transitions between terrains. Additionally, the fine tuning of the algorithm needs to account for navigation solutions due to heading changes. This will also incorporate tuning further parameters of the ZVU algorithm to include measurement noise, use with filtering algorithms, and multiple ZVU updates within a single ZVI.

Supplementary Materials: Not applicable.

Author Contributions: Conceptualization, T.K. and P.G.; investigation, T.K.; methodology, T.K.; software, T.K.; validation, T.K.; formal analysis, T.K.; investigation, T.K.; resources, T.K.; data curation, T.K.; writing—original draft preparation, T.K.; writing—review and editing, P.G.; visualization, T.K.; supervision, P.G.; project administration, T.K.; funding acquisition, T.K. All authors have read and agreed to the published version of the manuscript.

Funding: This research is funded by Northrop Grumman Corporation, the employer of T.K.

Institutional Review Board Statement: Not applicable.

Informed Consent Statement: Informed consent was obtained from all subjects involved in the study.

Data Availability Statement: The raw data supporting the conclusions of this article will be made available by the authors on request.

Acknowledgments: Not applicable.

Conflicts of Interest: The authors declare no conflict of interest.

References

1. Beaugregard, S.; Haas, H. Pedestrian dead reckoning: A basis for personal positioning. In Proceedings of the 3rd Workshop on Positioning, Navigation, and Communication, Hanover, Germany (16 March 2006).
2. Rahn, V.X.; Zhou, L.; Klieme, E.; Arnrich, B. Optimal Sensor Placement for Human Activity Recognition with a Minimal Smartphone-IMU Setup. *SENSORNETS*. **2021**, pp. 37–48.
3. Groves, P. *Principles of GNSS, Inertial, and Multisensor Integrated Navigation Systems*, 2nd ed.; Artech House: London, United Kingdom, 2013; pp. 240–245; pp. 638–641.
4. Zampella, F.; Khider, M.; Robertson, P.; Jiménez, A.; Unscented Kalman filter and magnetic angular rate update (MARU) for an improved pedestrian dead-reckoning. In Proceedings of the 2012 IEEE/ION Position, Location and Navigation Symposium, Myrtle Beach, United States (23 April 2012).
5. Abdulhahim, K.; Moore, T.; Hide, C.; Hill, C. Understanding the performance of zero velocity updates in MEMS-based pedestrian navigation. *International Journal of Advancements in Technology* **2014**, *5*(2).
6. Park, S.K.; Suh, Y.S. A zero velocity detection algorithm using inertial sensors for pedestrian navigation systems. *Sensors* **2010**, *10*(10), pp. 9163–9178.
7. Xing, H.; Li, J.; Hou, B.; Zhang, Y.; Guo, M. Pedestrian stride length estimation from IMU measurements and ANN based algorithm. *Journal of Sensors* **2017**, 2017.
8. Scott, S.H.; Winter, D.A. Biomechanical model of human foot; kinematics and kinetics during the stance phase of walking. *Journal of biomechanics* **1993**, *26*(9), pp. 1091–1104.
9. Mills, P.M.; Barrett, R.S. Swing phase mechanics of healthy and young and elderly men. *Human movement science* **2001**, *20*(4-5), pp. 427–446.
10. Murray, M.P.; Drought, A.B.; Kory, R.C. Walking patterns of normal men. *Journal of bone and joint surgery* **1964**, *46*(2), pp. 335–360.
11. Gast, K.; Kram, R.; Riemer, R. Preferred walking speed on rough terrain: is it all about energetics? *Journal of experimental biology* **2019**, 222(9).
12. Schwartz, R.P.; Heath, A.L.; Morgan, D.W.; Towns, R.C. A quantitative analysis of recorded variables in the walking patterns of “normal” men. *Journal of bone and joint surgery* **1964**, *46*(2), pp. 324–334.
13. Gao, H.; Groves, P.D. Context determination for adaptive navigation using multiple sensors on a smartphone. In Proceedings of the 29th International Technical Meeting of The Satellite Division of the Institute of Navigation (ION GNSS+ 2016), Portland, United States (16 September 2016).
14. Knuth, T.; Groves, P. IMU Based Context Detection of Changes in Terrain Topography. In Proceedings of the 2023 IEEE/ION Position, Location, and Navigation Symposium (PLANS), Monterrey, United States (24 April 2023).
15. Godha, S.; Lachapelle, G.; Cannon, E. Integrated GPS/INS system for pedestrian navigation in a signal degraded environment. In Proceedings of the 19th International Technical Meeting of the Satellite Division of the Institute of Navigation (ION GNSS), Fort Worth, United States (26 September 2006).
16. Feliz Alonson, R.; Zalama Casanova, E.; Gómez García-Bermejo, J. Pedestrian tracking using inertial sensors. *Journal of Physical Agents* **2009**, *3*(1), pp. 35–43.
17. Bird, J.; Arden, D. Indoor navigation with foot-mounted strapdown inertial navigation and magnetic sensors [emerging opportunities for localization and tracking]. *IEEE Wireless Communications* **2011**, *18*(2), pp. 28–35.
18. Fourati, H.; Manamanni, N.; Afilal, L.; Handrich, Y. Position estimation approach by complementary filter-aided IMU for indoor environment. In 2013 European Control Conference (ECC). Zurich, Switzerland (17 July 2013).
19. Darci, O.; Kuo, A.D. Humans plan for the near future to walk economically on uneven terrain. *Proceedings of the National Academy of Sciences* **2023**, *120*(19), p. e2211405120.
20. Voloshina, A.S.; Kuo, A.D.; Daley, M.A. Biomechanics and energetics of walking on uneven terrain. *Journal of Experimental Biology* **2013**, *216*(21). Pp. 3963–3970.
21. Hu, B.; Dixon, P.C.; Jacobs, J.V.; Dennerlein, J.T.; Schiffman, J.M. Machine learning algorithms based on signals from a single wearable inertial sensor can detect surface-and age-related differences in walking. *Journal of biomechanics* **2018**, *71*, pp. 37–42.
22. Nilsson, J.O.; Skog, I.; Händel, P.; Hari, K.V. Foot-mounted INS for everybody-an open-source embedded implementation. In Proceedings of the 1012 IEEE/ION Position, Location and Navigation Symposium, Myrtle Beach, United States (23 April 2012).
23. Wahlström, J.; Skog, I. Fifteen years of progress at zero velocity: A review. *IEEE Sensors Journal* **2020**, *21*(2), pp. 1139–1151.
24. Strozzi, N.; Parisi, F.; Ferrari, G. Impact of on-body IMU placement on inertial navigation. *IET Wireless Sensor Systems* **2018**, *8*(1), pp. 3–9.
25. Gupta, A.K.; Skog, I.; Händel, P. Long-term performance evaluation of a foot-mounted navigation device. In Proceedings of 2015 Annual IEEE India Conference (INDICON) New Delhi, India (17 December 2015).
26. Wentworth, C.K. A scale of grade and class terms for clastic sediments. *The journal of geology* **1922**, *30*(5), pp. 377–392.

Disclaimer/Publisher’s Note: The statements, opinions and data contained in all publications are solely those of the individual author(s) and contributor(s) and not of MDPI and/or the editor(s). MDPI and/or the editor(s) disclaim responsibility for any injury to people or property resulting from any ideas, methods, instructions or products referred to in the content.